



UNIVERSIDADE ESTADUAL DE CAMPINAS  
SISTEMA DE BIBLIOTECAS DA UNICAMP  
REPOSITÓRIO DA PRODUÇÃO CIENTÍFICA E INTELLECTUAL DA UNICAMP

**Versão do arquivo anexado / Version of attached file:**

Versão do Editor / Published Version

**Mais informações no site da editora / Further information on publisher's website:**

<https://saemobilus.sae.org/content/2016-36-0348>

**DOI: 10.4271/2016-36-0348**

**Direitos autorais / Publisher's copyright statement:**

©2016 by SAE International. All rights reserved.

DIRETORIA DE TRATAMENTO DA INFORMAÇÃO

Cidade Universitária Zeferino Vaz Barão Geraldo

CEP 13083-970 – Campinas SP

Fone: (19) 3521-6493

<http://www.repositorio.unicamp.br>



2016-36-0348

# Evaluation of Energy Recovery Potential through Regenerative Braking for a Hybrid Electric Vehicle in a Real Urban Drive Scenario

**André de Moura Oliveira**

State University of Campinas - UNICAMP

**Elvis Bertoti**

State University of Campinas - UNICAMP

**Jony Javorski Eckert**

State University of Campinas - UNICAMP

**Rodrigo Yassuda Yamashita**

State University of Campinas - UNICAMP

**Eduardo dos Santos Costa**

State University of Campinas – UNICAMP

**Ludmila Corrêa de Alkmin e Silva**

State University of Campinas - UNICAMP

**Franco Giuseppe Dedini**

State University of Campinas – UNICAMP

Copyright © 2016 SAE International

## Abstract

The need for improved fuel economy for road vehicles has increased the interest in hybrid electric vehicle (HEV) and recovering vehicle energy. This paper aims to evaluate the amount of kinetic energy that could be restored through regenerative braking in a HEV. This work will not resort the Brazilian urban driving cycle NBR 6601, for this cycle does not fully represent a pattern of traffic faced regularly in urban areas, which is typically composed of heavy traffic and long periods of idleness. Therefore, a new drive cycle will be developed that better represents the Brazilian traffic. Also, considering the shortage of energy resources, the large amount of energy dissipated as heat during braking a vehicle is a recurring concern. Therefore, measuring the maximum available energy that could be restored through regenerative braking is the first step towards estimating the profit of using this technology and how it would pay off the investment in the long run. Thus, a longitudinal vehicle dynamics model is implemented using MATLAB/Simulink in order to simulate a small-size hybrid vehicle undergoing the cycle set up and assess the energy balance looking forward to the energy available for recovery.

## Introduction

The shortage of fossil energy resources around the world likewise the concern about the pollutants expelled from the exhaust as a consequence of the combustion of petroleum derivatives have increased the interest on vehicular efficiency. High-efficient engines, kinetic energy recovery systems and hybrid electric vehicles are some of the alternatives to mitigate this issue. Specially, HEVs offers an acceptable solution for: improving the vehicle acceleration performance, rising the climbing capacity and reducing the engine fuel consumption [1].

HEVs allow different arrangements of internal combustion engines (ICE) and electric motors (EM) [2] and they are classified according to theirs power sources configuration. Series HEVs are propelled only by the EM, in which the ICE provides power to a generator that recharges the battery [3]. On the other hand, Parallel HEVs uses a combination of ICE and EMs (mechanically connected) to provide the required power to the vehicle [4]. Series - parallel hybrid combines the characteristics of both configurations using the ICE to propel the vehicle and also to charge the battery that supplies the electric propulsion system [5].

An advantage of electrified drivelines dwells in the fact that regenerative braking may also be employed to increase fuel economy and vehicle autonomy, especially in urban areas of heavy traffic [3]. Regenerative braking is a mechanism that converts, by means of an EM, part of the kinetic energy of the vehicle, while it decelerates, into electric energy. The converted energy is then used to recharge the energy storage systems (such as batteries and supercapacitors) and may be used in another convenient occasion [6], [7] and [8].

Furthermore, a few countries are creating some legislation aiming to stimulate the industries to enhance vehicle efficiency. Among these is Brazil that decreed in 2012 the INOVAR-AUTO [9], a law that reduces the (IPI), a tax for industrialized products, for automobiles to be sold in 2017. The vehicles shall consume 15.46% less than in 2011 in order to have a 1% discount of the IPI. If the automaker manages to increase the efficiency beyond 18.84%, the vehicle will receive a 2% discount, and in case of it does not reach the target, there is a penalization by increasing the IPI charged on that vehicle [10].

To quantify the enhancements in efficiency of the new produced vehicles, some standardized drive cycles were developed, which depend on a considerable set of parameters such as traffic condition, topography and characteristics of the driver [11].

This paper quantifies the amount of energy available for recovering in a hypothetical HEV equipped with regenerative braking, evaluated in a real-world drive pattern collected in the city of Campinas with the help of a Global Positioning System (GPS) navigation equipment, which measured and stored simultaneously both the altimetry and the speed profiles. The energy flux of the vehicle was obtained by means of simulations performed with a vehicle model in Matlab/Simulink™ for a HEV that presents engine and powertrain similar to a conventional 1.0L Brazilian vehicle.

## Vehicle Dynamics

Normally, vehicle dynamics may be divided into three large areas: longitudinal, vertical and lateral dynamics. Longitudinal dynamics has a higher influence on traction. Vertical dynamics is directly linked with the user comfort, but, also, has an influence on handling and traction due to the weight distribution. Lateral dynamics is extremely important for handling and stability study. As previously mentioned, this work focuses on longitudinal dynamics, consequently on the traction behavior of the HEV and its influence on the energy recovery.

In this paper, the vehicle dynamics is modeled mostly according to the equations presented by [12]. Figure 1 shows the forces that act over the vehicle, while it is moving.

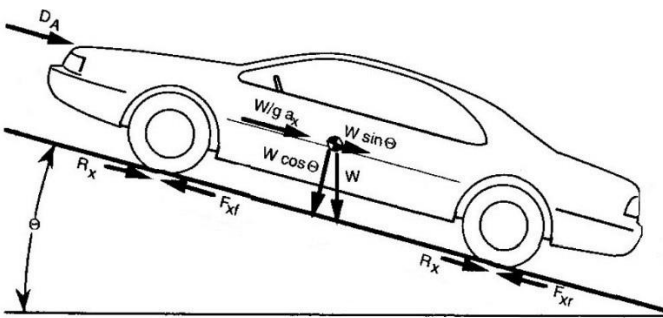


Figure 1 - Vehicle movement resistance forces adapted from [12]

The driver behavior (drive cycle) is defined by a speed profile which is used as target to define the vehicle required acceleration  $a_{req}$  [m/s<sup>2</sup>]. The acceleration, then, is defined in a feedback model, which is presented in the following section, by the difference between the cycle speed  $V_c$  [m/s] and the vehicle current speed  $V$  [m/s] divided by the simulation step  $dt$  [s].

$$a_{req} = \frac{V_c - V}{dt} \quad (1)$$

Once the required acceleration is defined, the vehicle traction force on the wheels  $F_{req}$  [N] is obtained by Equation (2) as a function of the vehicle mass  $M$  [kg], aerodynamic drag  $D_A$  [N], tire rolling resistance ( $R_x$ ) [N] and the influence of the road grade.

$$F_{req} = Ma_{req} + R_x + D_A + W \sin(\theta) \quad (2)$$

The road gradient presents significant influence over the vehicle dynamics, by varying the climbing resistance, which corresponds to the vehicle weight  $W$  [N] (force component parallel to the road plane), and it is a function of the road angle  $\theta$  [rad]. On uphill, the climbing resistance force acts against the movement; on the other hand, at downhill, the force acts in favor of the movement [12].

The aerodynamic drag  $D_A$  represents the resistance imposed by the air during the vehicle passage through the fluidic stream. This load is estimated by Equation (3) in function of the vehicle projected frontal area ( $A$ ) [m<sup>2</sup>], the density of the surrounding air ( $\rho$ ) [kg/m<sup>3</sup>], the drag coefficient ( $C_d$ ) [-], an empirical constant that varies according to the vehicle shape, and the vehicle's speed ( $V$ ) [m/s].

$$D_A = \frac{1}{2} \rho V^2 C_d A \quad (3)$$

For urban driving behavior, the tire rolling resistance ( $R_x$ ) [N] corresponds to a significant parcel of the vehicle power demand. This load results from the transformation of the mechanical energy into thermal energy due to deformation of the tire. Equation (4) shows an estimative of the rolling resistance as a function of the vehicle weight ( $W$ ) and the dimensionless rolling resistance coefficient ( $f_r$ ).

$$R_x = f_r W \quad (4)$$

The rolling resistance coefficient  $f_r$  is estimated as proposed by [13] and [14] as dependent of the vehicle speed ( $V$ ) [m/s], the vehicle weight ( $W$ ) [N], the tires inflation pressure  $p$  [Pa], and a constant  $K$ , which depends on type of the tire: 0.8 for radial and 1 for non-radial.

$$f_r = \frac{K}{1000} \left( 5.1 + \frac{5.5 \times 10^5 + 90W \cos(\theta)}{p} + \frac{1100 + 0.0388W \cos(\theta)}{p} V^2 \right) \quad (5)$$

After calculating the required force, one may determine the engine required torque  $T_{req}$  [Nm] by means of Equation (6), considering the gearbox and differential transmission ratios  $N_g$  and  $N_d$ , respectively, their correspondent rotational inertias,  $I_g$  and  $I_d$ , the radius of the tire  $r$  [m] and the powertrain overall efficiency  $\eta_{gd}$ .

$$T_{req} = \frac{F_{req} r + ((I_g + I_d)(N_g N_d)^2 + I_d N_d^2 + I_w) \frac{ax}{r}}{N_g N_d \eta_{gd}} \quad (6)$$

The required engine torque  $T_{req}$  is then compared with the maximum engine torque curve (100% throttle curve) as shown in Figure 2. If the necessary torque is below the available torque at a given engine speed,

the engine output torque  $T_e$  [Nm] becomes the required value. On the other hand, when the torque necessities overcome the available torque, the engine provides the maximum torque value for the engine curve according to the current engine speed, decreasing the vehicle acceleration performance.

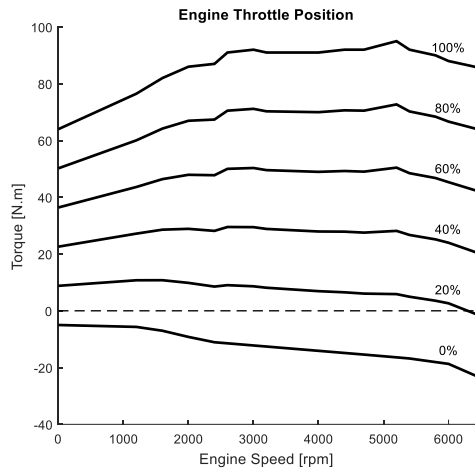


Figure 2 - Engine torque curves

Another possible situation happens when  $T_{req}$  results negative. In this occasion, the engine operates as engine brake limited to 0% of throttle curve. If the vehicle requires more brake torque than the engine and the driveline can deliver,  $T_e$  must be converted to its value at the wheel, and the vehicle required traction torque must be subtracted by it, as shown in Equation (7).

$$T_b = F_{req}r - T_e N_g N_d \eta_{gd} \quad (7)$$

Then, the vehicle current traction force  $F_x$  [N] delivered by the engine to the wheels is calculated by the Equation (8), as a function of the engine and power brake supplied torques  $T_e$  and  $T_b$ , respectively.

$$F_x = \frac{T_e N_g N_d \eta_{gd} - T_b}{r} \quad (8)$$

The vehicle acceleration ( $a_x$ ) [m/s<sup>2</sup>] is later determined directly by the Equation (9).

$$a_x = \frac{F_x - R_x - D_A - W \sin(\theta)}{M + ((I_e + I_g)(N_g N_d)^2 + I_d N_d^2 + I_w)} \quad (9)$$

### Vehicle modeling

In order to stipulate the energy recovery potential in a drive cycle, a Simulink™ model was developed. A simplified version of the model excepting some signal outputs may be seen in Figure 3.

For the development, the longitudinal dynamics equations described in the previous sections were subdivided and implemented in block diagram logic of Simulink™ in the following sequence as follow:

- Inputs: for the execution, the model requires the speed profile of the vehicle along the drive cycle and the road gradient, both as a function of time;
- Driver: it calculates the required torques at the wheel and at the engine and outputs the actuating signals for the engine, gearbox and brake blocks (Equations 1 to 7);
- Engine: in this block are implemented two torque limiters, which prevents the engine from outputting more torque than it actually can deliver and less torque than the engine friction may provide. A null input means that the engine operates in full engine brake mode (0% throttle), without fuel consumption, and a 1 input means full torque (100% throttle). This block is also responsible for computing the instantaneous fuel consumption of the vehicle by means of a brake specific fuel consumption map (BSFC). The engine block outputs torque and its internal inertia;
- Clutch: this block was modeled as if the clutch disks were always coupled. In other words, for this model the time required for a gear shifting was not considered and it would require further development. Then, clutch outputs have the same torque and inertia of the engine;
- Gearbox: it receives the information of which gear should be engaged according to the gear shifting strategy proposed by [15], and it uses the gear ratio and inertia of the respective gear couple to amplify the input torque and inertia;

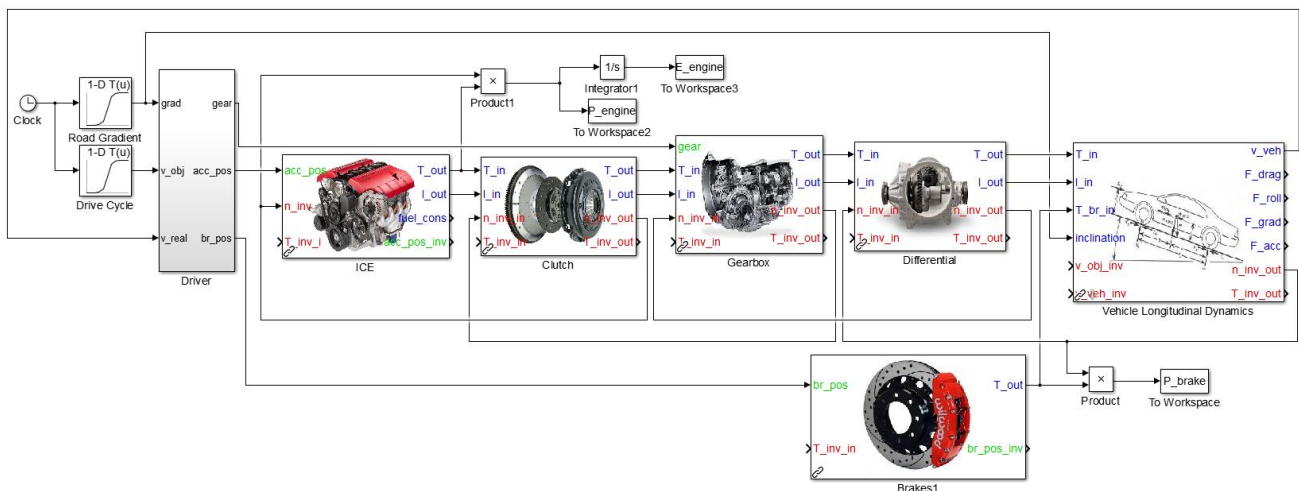


Figure 3 - Simplified Simulink Model

- **Differential:** here the constant gear ratio and rotational inertia are used and the same calculation of the gearbox is employed for performing the torque and inertia amplification. Then, the amplified torque is multiplied by the driveline efficiency, which simulates the losses in the whole powertrain due to friction and heat;
- **Brake:** converts the input signal into braking torque, meaning null absence of braking torque and 1 the maximum amount of torque that all four wheels can deliver;
- **Vehicle Longitudinal Dynamics:** in this block, the torque is converted into a force at the wheel and then deducted from rolling, air and climbing resistances. After the computation of the resultant force, the rotational inertia is converted into linear inertia and summed with the total mass of the vehicle. With these parameters the block determines the acceleration of the vehicle (Equations 8 and 9), which is integrated to output the vehicle's speed. Afterwards, this signal is sent to the Driver block, so it can be recalculated in the next positions for the actuators.

The angular velocity of the rotating components follows the inverse logic, since it depends on the vehicle speed. Therefore, its signal must start from the Longitudinal Dynamics block and pass through all the previous components until the engine rotational speed may be calculated.

The main information that is obtained with this model are the power signals (torque times angular velocity) of the engine ( $P_{engine}$ ), brakes ( $P_{brake}$ ) and the integration of  $P_{engine}$  in time, and the mechanical energy delivered by the engine ( $E_{engine}$ ). Since the main goal of the present work is to measure the whole recuperation potential, independent of the employed hybrid configuration and its efficiency, the brake power was then redistributed into the power that must be supplied by the friction brakes and the power that would be recovered by the electric motor if the electric propulsion system was 100% efficient.

By doing this, one may take into account the recuperation potential as a function of the hybridization level, which is the ratio between the EM power and the ICE power. In the situation that the vehicle demands more braking power than the electric motor can deliver, the friction brakes must be activated.

The values employed in the simulations are synthetized in Table 1.

Table 1 - Simulated Vehicle Parameters [16]

Variables	Symbol	Units	Values				
Air density	$\rho$	kg/m <sup>3</sup>	1.2922				
Differential inertia	$I_d$	kgm <sup>2</sup>	9.22E-04				
Differential ratio	$N_d$	-	4.87				
Drag Coefficient	$C_d$	-	0.33				
Engine inertia	$I_e$	kgm <sup>2</sup>	0.1367				
Frontal Area	$A$	m <sup>2</sup>	1,8				
Gearbox Speeds	-	-	1 <sup>st</sup>	2 <sup>nd</sup>	3 <sup>rd</sup>	4 <sup>th</sup>	5 <sup>th</sup>
Gearbox inertia	$I_g$	kgm <sup>2</sup>	0.0017	0.0022	0.0029	0.0039	0.0054
Gearbox ratios	$N_g$	-	4.27	2.35	1.48	1.05	0.8
Overall Efficiency	$\eta_{gd}$	-	0.9				
Tire inflation press.	$p$	Pa	2.0684 · 10 <sup>5</sup>				
Tire roll. res. coeff.	$K$	-	1.0				
Tires radius	$r$	m	0.2876				
Wheels inertia	$I_w$	kgm <sup>2</sup>	2.00				

## Drive Cycle

The fuel economy of a vehicle is largely affected by the drive cycle over which it is tested [17]. Therefore, employing a cycle that does not resemble the type of traffic that is being studied might induce to inaccurate results.

This paper emphasizes the traffic found regularly in urban areas, which may be characterized by low speed, low engine load, and low exhaust gas temperature [18] and it is composed of low average speeds, long periods of idleness and frequent stops. A driving situation like this is especially positive for regenerative braking implementation, as regenerative braking manages to provide the majority of the total braking force during low speed and stop-and-go traffic where most of deceleration is required [19].

Studies related to Brazilian traffic commonly resort to the Brazilian cycle NBR 6601 (Figure 4), which was developed experimentally and is usually employed on evaluations of vehicular emissions in a chassis dynamometer [20].

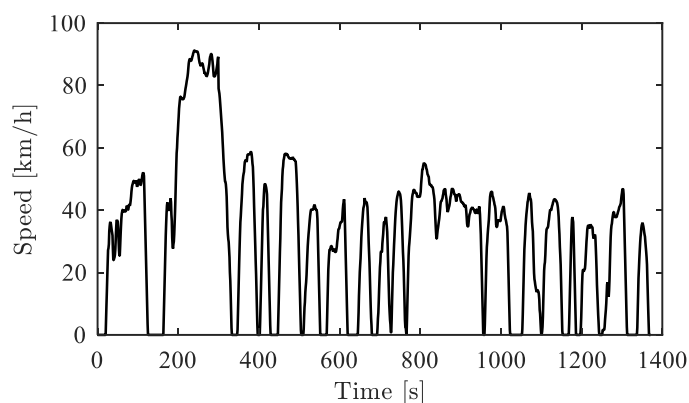


Figure 4 - NBR 6601 driving cycle [20]

However, this cycle presents some shortcomings if employed for other kinds of analyses related to urban areas. For instance, in the cycle NBR 6601 the average speed is of 31.6 km/h and the vehicle remains idle for just 13.8% of the time. In general, urban drive cycles exhibit percentage of time in idleness and average speed quite discrepant from the mentioned cycle. For instance, the European Urban Drive Cycle (ECE-15), EPA New York City Cycle (NYCC) and the Japanese 08 mode (JC08), all urban cycles, have as percentage of time in idleness 23.08%, 31.10% and 28.70%, respectively. Also, these cycles present inferior values for average speed. Respectively, 18.4 km/h, 11.5km/h and 24.4 km/h [21] and [22]. These data are resumed in Table 2.

Table 2 - Drive Cycles parameters [21]

Drive cycle	Total Distance (km)	Total Time (s)	Avg. Speed (km/h)	% of time idling	% of time braking
<b>ECE-15</b>	0.9946	195	18.4	23.08%	20.51%
<b>NYCC</b>	19.0276	598	11.5	31.10%	21.57%
<b>JC08</b>	8.171	1204	24.4	28.7%	33.6%
<b>NBR 6601</b>	11.997	1369	31.6	13.81%	19.8%

Moreover, the standardized drive cycles does not include gradient, which is a quite relevant variable since, according to the principle of conservation of mechanical energy, the energy required to upraise an

acclivity of 40 m (a habitual acclivity even in not so hilly areas) is equivalent to the energy required to speed up the vehicle from zero to 100 km/h. Exemplifying, this means that to maintain the vehicle speed during descents, a vehicle without regenerative braking waste more energy than in a plane route.

Therefore, in order to have a reliable drive cycle that corresponds to the form of traffic found in large cities, a new cycle was developed in the urban area of Campinas in Brazil. Campinas is the third most populous city of São Paulo State, with more than 1,150,000 inhabitants. From 2000 to 2014 Campinas saw an increase of 98.3% of its automotive fleet, reaching 881.235 vehicles, while its population grew only 19.1% during the same period [23]. This leads to a common growing issue in large cities: frequent traffic jams. Precisely the condition of traffic that distinguishes an urban traffic state from the others and which should definitely account for an urban drive cycle, although it is not represented accordingly in the NBR 6601 cycle.

### Data acquisition for Real Driving Cycle

According to [24], approximately 72% of Campinas' fleet is composed of passenger cars and unlike other vehicle types such as public busses or heavy freight vehicles (which are almost fully restricted to expressways), passenger cars generally utilize all kind of roads [25]. Thus, a route containing diversified roadways of Campinas was set up, covering highly utilized freeways, arterial, collectors and local roads [26]. The roadways were selected to better suit the traffic conditions of the city in terms of usage, speed profile, travel patterns (home-to-work, mainly) and topography [27].

Aiming an even more consistent drive cycle for urban areas, the time selected to perform data acquisition was from 5:00 p.m. until 7:30 p.m. This choice was made mainly because of the substantial amount of daily trips which are made from home-to-work and vice-versa [25] and are largely made in this peak period, as observed in the statistics data of Maplink Traffic for Campinas city [28].

Maplink is a Brazilian company specialized at providing geo-location services and real-time routing in roads and cities for companies. Also, real-time traffic conditions monitoring through Google Maps online was used to establish the selected time.

The time length of the drive cycle was also taken into account when evaluating the cycle. According to a survey performed by FIRJAN, in large Brazilian cities as Rio de Janeiro, São Paulo and Belo Horizonte, the average time spent in traffic per day is equivalent to 141, 132 and 125 minutes, respectively [29]. A more recent research, conducted by IBOPE in 2014, reveals that vehicle drivers of São Paulo spent, in average, 104 minutes in traffic per day on work-home-work trips and 168 minutes considering all micro trips performed in a regular day, such as going to the market, a gym, restaurants, etc. [30]. The developed cycle in this paper, exhibits a time span of, approximately, 125 minutes, thus being coherent with the average time spent in the traffic of most Brazilian large cities.

This paper employs on-board measurement through an instrumented car with a GPS navigator to acquire and store real-world data of the chosen driving routes. The cycle contains the velocity profile associated to the road altimetry utilized to determine the road gradient. For data acquisition, the GlobalSAT™ 580p navigator was used, which allowed the exporting of the traveled route data to a file that might be imported by Matlab™ in order to generate the speed cycle and gradient files employed in the simulations.

The drive cycle starts at the State University of Campinas (UNICAMP), passing through Campinas' downtown and returning to the University along diversified roads (Figure 5). Thereby, variations on altitude won't account to the final energy balance, neither positively nor negatively, for it begins and ends at the same location, only being considered how the gradient affects instantly the potential energy for recovery and its relations with vehicle kinetics.

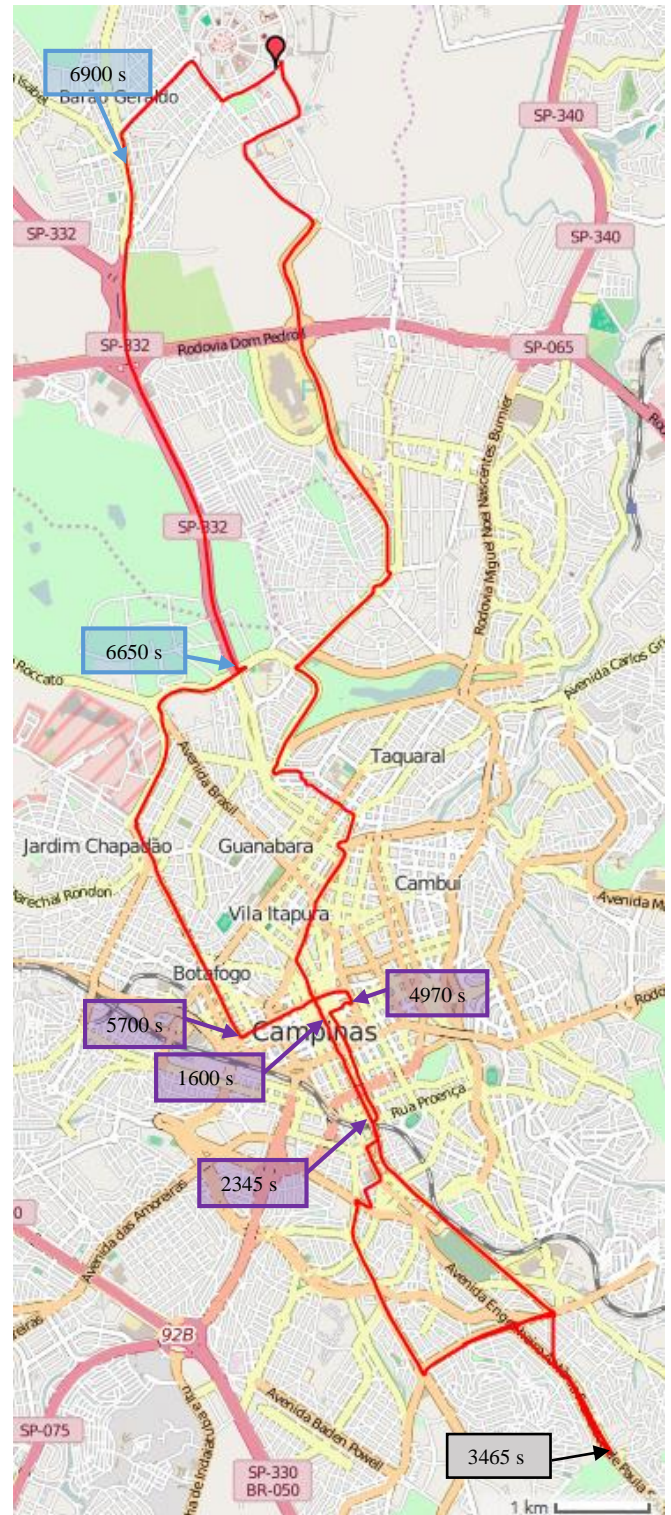


Figure 5 - Developed driving cycle map

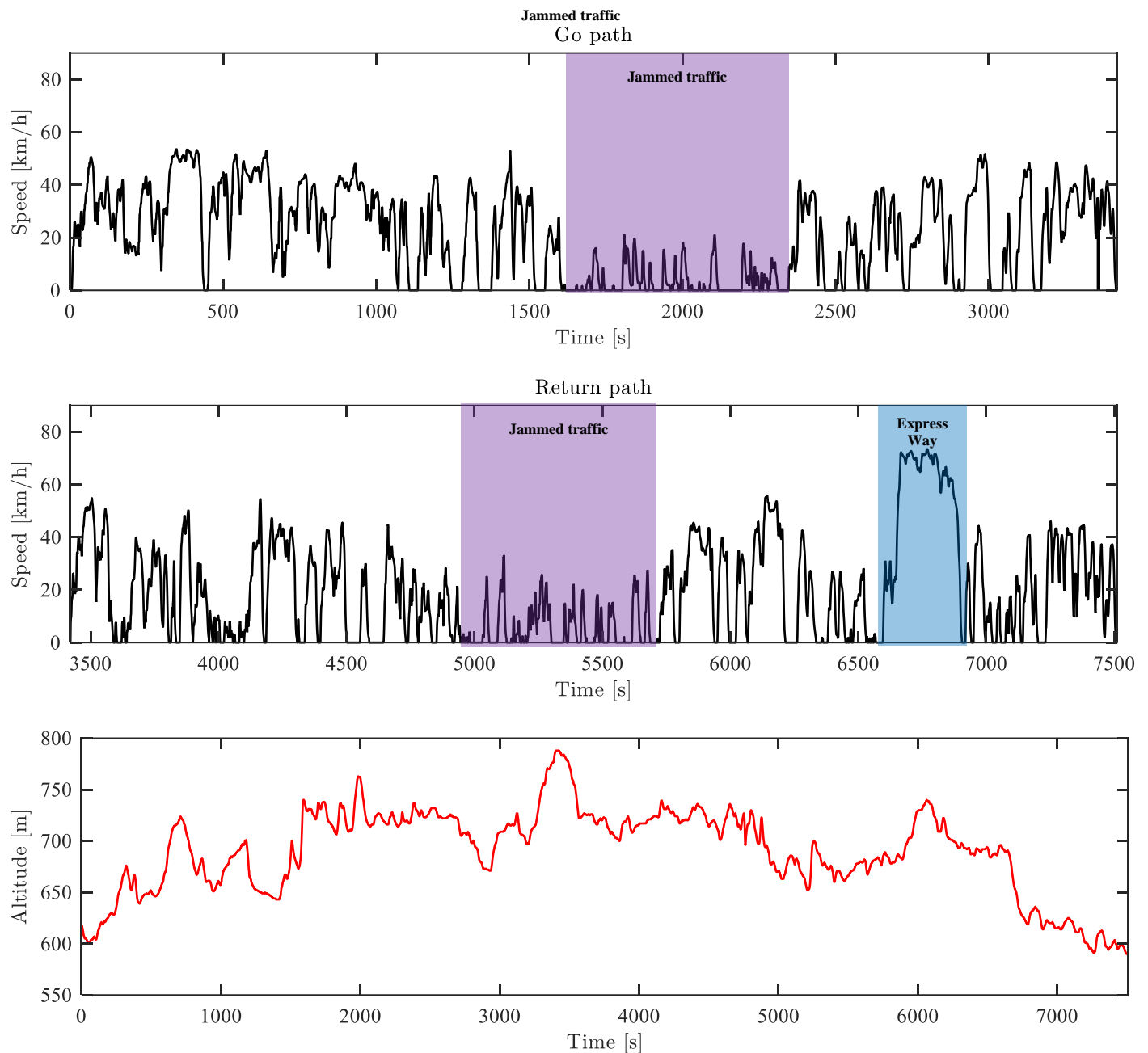


Figure 6 - Developed driving cycle

Observing Figure 6, it becomes clear that most part of the developed cycle occurs in an urban regime, as proposed earlier. Although, in home-to-work and work-to-home trips the driver faces other patterns of traffic, like the ones found in traffic jams and express ways. These different patterns are also present in the suggested cycle. For example, from 1600 s to 2345 s, there is an excerpt of traffic jam, characterized by a very low average speed and a long time of idleness. Furthermore, during the interval from 6650 s to 6900 s, the driver is traveling through an expressway, identified for its high average speed and no stops.

Also, the cycle presented, approximately, 25% of the time in braking regime and 23% in idleness, which are consistent with the data from other urban drive cycles shown in Table 2.

The cycle was divided into two steps with a target place to go, and the return path. As could be observed in Figure 5 and Figure 6, the return path starts at 3465 s, which corresponds to the highest altimetry point presented in the proposed driving cycle.

## Simulation results

For comparison purposes, simulations routines were performed for both the cycle developed in this paper and for the NBR 6601 cycle. As proposed, this paper aims to evaluate the amount of energy that could be recovered through regenerative braking, thus, the results are presented as percentage of spent energy in comparison with the energy of the driveline.

Three different vehicle masses, of 1200 kg, 1350 kg and 1500 kg, were employed in the simulations in order to assess the possible effect of the weight over the regeneration potential: the first configuration takes into account only the weight of a mild hybrid implementation (approximately, 150 kg [31]) plus the driver; the second configuration considers the adding of two passengers; the third refers to a loaded vehicle.

A hybridization of 10 kW [32] of the vehicle total power was considered for the regenerative braking, in order to illustrate possible weaknesses of HEVs. This corresponds to a 14.78% of hybridization, which matches with a mild hybrid configuration. Since the HEV configuration is not relevant for this paper, the full regeneration potential can be easily obtained by summing the energy rejected by the brakes with the energy recovery by the 10 kW electric propelling system. Other vehicles features are listed in Table 1.

Figure 7 and Table 3 show the results obtained for the simulations along the NBR 6601.

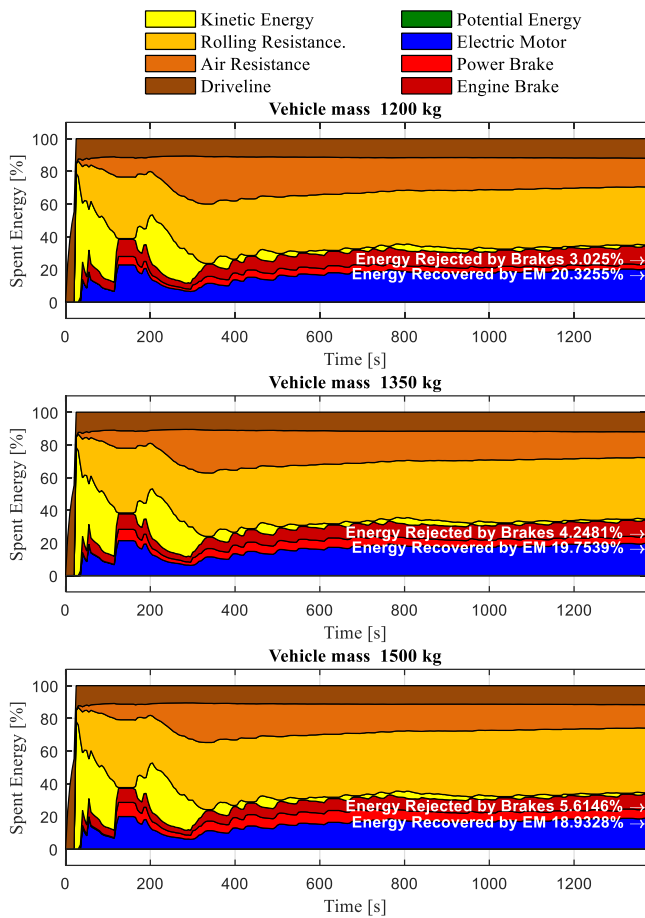


Figure 7 - NBR 6601 results

Table 3 - NBR 6601 results

Vehicle mass (kg)	Energy Rejected by Brakes (%)	Energy Recovered by EM (%)	Total Recuperation Potential (%)
1200	3.0250	20.3255	23.3505
1350	4.2481	19.7539	24.0020
1500	5.6146	18.9328	24.5474

The results obtained for the developed cycle are shown in Figure 8 and synthesized in Table 4.

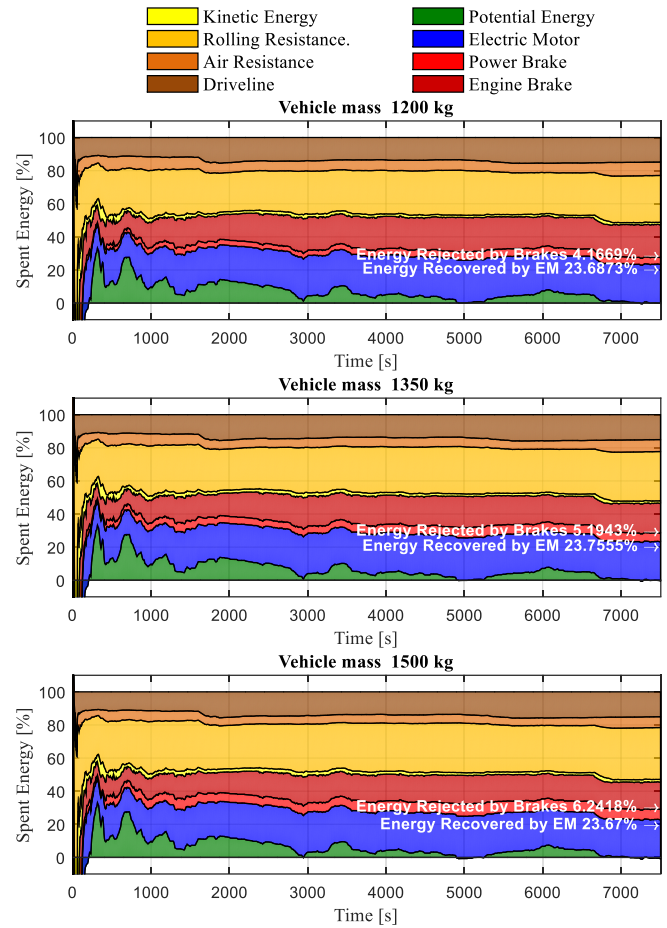


Figure 8 - Campinas cycle results

Table 4 - Campinas cycle results

Vehicle mass (kg)	Energy Rejected by Brakes (%)	Energy Recovered by EM (%)	Total Recuperation Potential (%)
1200	4.1669	23.6873	27.8542
1350	5.1943	23.7555	28.9493
1500	6.2418	23.6700	29.9118

It is noticeable that an increase of the vehicle total mass affects positively the full recuperation potential, which is the energy rejected by the brakes added to the energy recovered by the EM. For instance, in the real cycle driven through Campinas, the recoverable energy for the 1200 kg vehicle case resulted 27.85%, while, for the 1500 kg case, the total recoverable energy resulted 29.92%, a variation of more than two percentage points of the total mechanical energy produced by the engine.

Although, this increase leads to an equal or inferior percentage of energy that could be regenerate by a vehicle provided with a limited electrification power, which is also observable in both Table 3 and Table 4. This occurs due to the harder decelerations forces that surpass the ability of the EM of supplying the total brake torque for the wheels, requiring more power to be delivered by the friction brakes and consequently wasting more energy.

In order to increase the recoverable energy, an electric system with more power might be employed. This goal could be reached by increasing the hybridization level of the vehicle, or by adding a storage system with higher specific power, such as flywheels.

There are studies showed the synergy of a system in which chemical batteries work together with flywheels as energy storage elements. Moreover, flywheels have longer life than chemical batteries, helping the hybrid system to have a longer life span in comparison with HEVs with only batteries as energy storage system.

It is also observable that the cycle developed in this paper through the city of Campinas presented a higher percentage of recoverable energy than the NBR 6601 cycle for every case. In average, both the total recuperation potential and the HEV configuration with power limitations resulted 20.6% higher in the real cycle than for the NBR 6601, as expected.

The regenerative braking also reduces the use of the HEV frictional brakes, as compared with a conventional vehicle as shown in Table 5. The use of the EM system as generator is mostly enough to fulfill the cycles required brake torque, minimizing the use of the frictional brakes that are used only when the EM system regenerative capacity is below the required braking torque. Even in this situation, the vehicle brakes system is less required because the EM continues regenerating at maximum capacity during the use of the mechanical braking system. It was observed an increase in the use of the friction brakes with the HEV mass increase, because the higher mass HEV more easily exceeds the EM regenerative torque capacity.

Table 5 - Friction Brake use in the simulated driving cycles

Vehicle	NBR 6601 Friction Braking		Campinas Cycle Friction Braking	
	[s]	[%]	[s]	[%]
Conv. 980 kg	234.40	17.10	1901.5	25.32
HEV 1200 kg	68.00	4.96	232.15	3.09
HEV 1350 kg	95.80	6.99	285.30	3.80
HEV 1500 kg	111.90	8.16	354.90	4.73

Even though not being the purpose of this paper, it is visible in Figure 7 and Figure 8 that rolling resistance corresponds to the majority of the energy losses. Therefore, optimization researches covering this subject are strongly relevant for further improvements in fuel economy.

## Conclusions

In this paper the potentiality of regenerative braking for a HEV driving in urban conditions was studied. A Simulink™ model was developed to simulate the vehicle longitudinal dynamics, and the recuperation potential (ratio between the regained energy and the total mechanical energy produced by the engine) are compared for three HEV mass configurations running along two different driving cycles: the NBR 6601 and a drive pattern, which was obtained in a run during the rush hour across the city of Campinas in Brazil. The real data was acquired with help of a navigator with embedded Global Position System (GPS) capability.

The results compared the Brazilian Urban cycle NBR 6601 and a new urban driving cycle developed for the driving behavior in the city of Campinas in Brazil have shown that the chosen drive pattern may have strong influence over the recuperation potential. As an example, the proposed drive cycle had a recuperation potential of around 20% higher than the standardized NBR 6601, which has higher average speeds and less idling time. This difference provides evidence why governments and automakers should pay great attention to this variable, when assessing the real gains that could be obtained by the electrification of the driveline. Real drive patterns obtained from statistical approaches may come into help on this subject.

Furthermore, the simulated HEV has shown a potential of 23.7% of energy recovery potential, with the electric motor limitation of 10 kW in power, and 28.9% of full recovery potential when performing the real driving cycle executed in the city of Campinas. However, these gains might be diminished by the efficiency of a real electrified powertrain, and this result expresses the significant benefits of employing hybridization, in a real urban Brazilian scenario, like in the city of Campinas. This technology, is still very incipient in Brazil, lessens significantly the impacts of tailpipe emissions by optimizing the fuel economy of the vehicle, representing not only an environmental advantage for the cities, but also an economical advantage for the owner.

Additionally heavier vehicles presented also, as expected, higher recuperation potentials when they are equipped with hybridized powertrains, however, these gains are highly limited by the hybridization level. As the study has shown, with a mild hybrid configuration of 14.78%, increasing the mass of the vehicle caused actually a decrease in the potential of recovery, since the power demanded for the deceleration surpassed the available electric power. In other words, the friction brakes must be actuated and energy must be wasted, showing that the hybridization level can be optimized according to the vehicle usage, in order to explore the full recuperation potential of a given drive pattern.

For further works, it is suggested the evaluation of the influence in fuel economy of the new drive cycle, as well as its impact in emissions.

## References

1. Yazdani, A, AH Shamekhi, and SM Hosseini. 2015. "Modeling, performance simulation and controller design for a hybrid fuel cell electric vehicle." *Journal of the Brazilian Society of Mechanical Sciences and Engineering* no. 37 (1):375-396.
2. Ehsani, Mehrdad, Yimin Gao, and Ali Emadi. 2009. "Modern electric, hybrid electric, and fuel cell vehicles: fundamentals, theory, and design."
3. Souza, Reynaldo Barros de. 2010. "Uma visão sobre o balanço de energia e desempenho em veículos híbridos."
4. Schouten, Niels J, Mutasim A Salman, and Naim A Kheir. 2002. "Fuzzy logic control for parallel hybrid vehicles." *Control Systems Technology, IEEE Transactions on* no. 10 (3):460-468.
5. Rizoulis, Dimitrios, Jeffrey Burl, and John Beard. 2001. Control strategies for a series-parallel hybrid electric vehicle. SAE Technical Paper.
6. Kapoor, Radhika, and C Mallika Parveen. 2013. Comparative study on various KERS. Paper read at Proceedings of the World Congress on Engineering.

7. Junzhi, Zhang, Li Yutong, Lv Chen, and Yuan Ye. 2014. "New regenerative braking control strategy for rear-driven electrified minivans." *Energy Conversion and Management* no. 82:135-145.
8. Lv, Chen, Junzhi Zhang, Yutong Li, and Ye Yuan. 2015. "Mechanism analysis and evaluation methodology of regenerative braking contribution to energy efficiency improvement of electrified vehicles." *Energy Conversion and Management* no. 92:469-482.
9. INOVAR-AUTO. 2012. Programa de Incentivo à Inovação Tecnológica e Adensamento da Cadeia Produtiva de Veículos Automotores. [http://www.planalto.gov.br/CCIVIL\\_03/\\_Ato2011-2014/2012/Decreto/D7819.htm](http://www.planalto.gov.br/CCIVIL_03/_Ato2011-2014/2012/Decreto/D7819.htm).
10. Santiciolli, Fabio Mazzariol, Jony Javorski Eckert, Eduardo Dos Santos Costa, Heron José Dionísio, and Franco Giuseppe Dedini. 2013. Evaluation of Available Energy for Regenerative Breaking at the Brazilian Driving Cycle. SAE Technical Paper.
11. Schwarzer, Volker, and Reza Ghorbani. 2013. "Drive cycle generation for design optimization of electric vehicles." *Vehicle Technology, IEEE Transactions on* no. 62 (1):89-97.
12. Gillespie, Thomas D. 1992. *Fundamentals of Vehicle Dynamics*. Edited by Society of Automotive Engineers. 1<sup>st</sup> ed. Warrendale, Pa., USA.
13. Genta, Giancarlo. 1997. *Motor vehicle dynamics: modeling and simulation*. Vol. 43: World Scientific.
14. Jazar, Reza N. 2008. "Vehicle Dynamics." *Theory and Applications*. Riverdale, NY: Springer Science+ Business Media.
15. GM. 2013. Owner Manual Chevrolet Celta 2013. General Motors Brazil Ltda.
16. Eckert, Jony J, Fabio M Santiciolli, Ludmila CA Silva, Eduardo S Costa, Fernanda C Corrêa, and Franco G Dedini. 2016. "Co-simulation to evaluate acceleration performance and fuel consumption of hybrid vehicles." *Journal of the Brazilian Society of Mechanical Sciences and Engineering*:1-14.
17. Doucette, Reed T, and Malcolm D McCulloch. 2011. "A comparison of high-speed flywheels, batteries, and ultracapacitors on the bases of cost and fuel economy as the energy storage system in a fuel cell based hybrid electric vehicle." *Journal of Power Sources* no. 196 (3):1163-1170.
18. Lopes, M, L Serrano, I Ribeiro, P Cascão, N Pires, S Rafael, L Tarelho, A Monteiro, T Nunes, and M Evtugina. 2014. "Emissions characterization from EURO 5 diesel/biodiesel passenger car operating under the new European driving cycle." *Atmospheric Environment* no. 84:339-348.
19. Yoong, MK, YH Gan, GD Gan, CK Leong, ZY Phuan, BK Cheah, and KW Chew. 2010. Studies of regenerative braking in electric vehicle. Paper read at Sustainable Utilization and Development in Engineering and Technology (STUDENT), 2010 IEEE Conference on.
20. ABNT, NBR 6601. 2012. Light road motor vehicles - Determination of hydrocarbons, carbon monoxide, nitrogen oxides, carbon dioxides and particulate matter in the exhaust gas.
21. BARLOW, Tim J, S Latham, IS McCrae, and PG Boulter. 2009. *A reference book of driving cycles for use in the measurement of road vehicle emissions*.
22. Kühlwein, Jörg, German John, and Bandivadekar Anup. 2014. Development of test cycle conversion factors among worldwide light-duty vehicle CO<sub>2</sub> emission standards. The International Council on Clean Transportation - ICCT.
23. g1.globo.com. *Frota de veículos aumenta 93,8% em Campinas em 14 anos, aponta estudo*, 17/05 2016. Available from <http://g1.globo.com/sp/campinas-regiao/noticia/2015/09/frota-de-veiculos-aumenta-938-em-campinas-em-14-anos-aponta-estudo.html>.
24. IBGE, Instituto Brasileiro de Geografia Estatística. 2014 [cited 05/19/2016. Available from <http://cidades.ibge.gov.br/xtras/temas.php?lang=&codmun=350950&idtema=139&search=sao-paulo|campinas|frota-2014>.
25. Ho, Sze-Hwee, Yiik-Diew Wong, and Victor Wei-Chung Chang. 2014. "Developing Singapore Driving Cycle for passenger cars to estimate fuel consumption and vehicular emissions." *Atmospheric Environment* no. 97:353-362.
26. Prefeitura de Campinas. 2006. Plano Diretor Campinas. [http://www.campinas.sp.gov.br/governo/seplama/plano-diretor-2006/doc/tr\\_tracar.pdf](http://www.campinas.sp.gov.br/governo/seplama/plano-diretor-2006/doc/tr_tracar.pdf).
27. Sinfreicar, Sindicato das Empresas de Transportes de Passageiros por Fretamento de Campinas e Região 2010 [cited 05/20/2016. Available from <http://www.sinfreicar.org.br/portal/?p=4527>.
28. maplink. *Estatísticas de trânsito em Campinas* 2016 [cited 05/20/2016. Available from <http://maplink.com.br/SP/campinas/Estatisticas>.
29. FIRJAN, Federação das Indústrias do Estado do Rio de Janeiro *O custo dos deslocamentos nas principais áreas urbanas do Brasil* 2015 [cited 05/21/2016. Available from <http://www.firjan.com.br/lumis/portal/file/fileDownload.jsp?fileId=2C908A8F4F8A7DD3014FB26C8F3D26FE&inline=1>.
30. Fecomercio, Federação do Comércio do Estado de São Paulo; Ibope, Instituto Brasileiro de Pesquisa e Estatística. *1h44 é o tempo médio gasto pelo paulistano no trânsito na cidade* 2015 [cited 05/21/2016. Available from <http://www.fecomercio.com.br/noticia/1h44-e-o-tempo-medio-gasto-pelo-paulistano-no-transito-na-cidade>.
31. Eckert, Jony Javorski, Fernanda Cristina Corrêa, Fabio Mazzariol Santiciolli, Eduardo Dos Santos Costa, Heron José Dionísio, and Franco Giuseppe Dedini. 2014. Parallel Hybrid Vehicle Power Management Co-Simulation. SAE Technical Paper.
32. Costa, Eduardo Dos Santos, Jony Javorski Eckert, Fabio Mazzariol Santiciolli, Heron José Dionísio, Fernanda Cristina Corrêa, and Franco Giuseppe Dedini. 2014. Computational and Experimental Analysis of Fuel Consumption of a Hybridized Vehicle SAE Technical Paper.

## Contact Information

For additional information, contact André de Moura Oliveira at:  
 Integrated Systems Laboratory  
 Mechanical Engineering  
 State University of Campinas (UNICAMP)  
 Campinas, São Paulo, Brazil  
 mouraoliveira.andre@gmail.com

## Acknowledgments

This work was conducted during scholarships supported by the São Paulo Research Foundation (FAPESP), Brazilian Federal Agency for Support and Evaluation of Graduate Education (CAPES), National Council for Scientific and Technological Development (CNPq) and the State University of Campinas (UNICAMP).

## Definitions/Abbreviations

<b>BSFC</b>	brake specific fuel consumption	
<b>HEV</b>	Hybrid Electric Vehicle	
<b>NBR</b>	Brazilian standard	
<b>ICE</b>	Internal Combustion Engine	
<b>EM</b>	Electric Motor	
<b>INOVAR-AUTO</b>	Brazilian Law	
<b>IPI</b>	Brazilian Industrialized Products Tax	
<b>ECE</b>	European Urban Drive Cycle	
<b>EPA NYCC</b>	New York City Cycle	
<b>JC08</b>	Japanese Emission Test Cycle	
<b>FIRJAN</b>	Federação das Indústrias do Estado do Rio de Janeiro	
<b>IBOPE</b>	Instituto Brasileiro de Pesquisa e Estatística	
<b>GPS</b>	Global Positioning System	
<b>UNICAMP</b>	State University of Campinas	
$V_c$	Driving cycle speed	[m/s]
$V$	Vehicle speed	[m/s]
$dt$	Simulation step time	[s]
$a_{req}$	Vehicle requested acceleration	[m/s <sup>2</sup> ]
$F_{req}$	Requested traction force	[N]
$M$	Vehicle mass	[kg]
$D_A$	Aerodynamic drag	[N]
$R_x$	Rolling resistance	[N]
$W$	Vehicle weight	[N]
$\theta$	Road grade angle	[rad]
$A$	Vehicle frontal area	[m <sup>2</sup> ]
$\rho$	Air density	[kg/m <sup>3</sup> ]
$C_d$	Drag coefficient	
$f_r$	Rolling resistance coefficient	
$p$	Tires inflation pressure	[Pa]
$K$	Tire type constant	
$T_{req}$	Engine requested torque	[Nm]
$N_g$	Gearbox transmission ratio	
$N_d$	Differential transmission ratio	
$r$	Tire external radius	[m]
$\eta_{gd}$	Transmission overall efficiency	
$a_x$	Vehicle longitudinal acceleration	[m/s <sup>2</sup> ]
$I_e$	Engine inertia	[kgm <sup>2</sup> ]
$I_g$	Gearbox inertia	[kgm <sup>2</sup> ]
$I_d$	Differential inertia	[kgm <sup>2</sup> ]
$I_w$	Wheels and Tires inertia	[kgm <sup>2</sup> ]
$T_e$	Engine torque	[Nm]
$T_b$	Brake torque	[Nm]
$F_x$	Traction force	[N]

All rights reserved. No part of this publication may be reproduced, stored in a retrieval system, or transmitted, in any form or by any means, electronic, mechanical, photocopying, recording, or otherwise, without the prior written permission of SAE.

**ISSN 0148-7191**

**Copyright © 2016 SAE International.**

Positions and opinions advanced in this paper are those of the author(s) and not necessarily those of SAE. The authors solely responsible for the content of the paper.